Central depression of nuclear charge density distribution

Yanyun Chu (褚衍运),[1,*] Zhongzhou Ren (任中洲),[1,2] Zaijun Wang (王再军),[3] and Tiekuang Dong (董铁矿)[4]

[1]*Department of Physics, Nanjing University, Nanjing 210008, China*

[2]*Center of Theoretical Nuclear Physics, National Laboratory of Heavy-Ion Accelerator, Lanzhou 730000, China*

[3]*Department of Mathematics, Physics and Information Science, Tianjin University of Technology and Education, Tianjin 300222, China*

[4]*Faculty of Information Technology, Macau University of Science and Technology, Macau 999078, China*

(Received 4 July 2010; published 27 August 2010)

The center-depressed nuclear charge distributions are investigated with the parametrized distribution and the relativistic mean-field theory, and their corresponding charge form factors are worked out with the phase shift analysis method. The central depression of nuclear charge distribution of ^{46}Ar and ^{44}S is supported by the relativistic mean-field calculation. According to the calculation, the valence protons in ^{46}Ar and ^{44}S prefer to occupy the $1d_{3/2}$ state rather than the $2s_{1/2}$ state, which is different from that in the less neutron-rich argon and sulfur isotopes. As a result, the central proton densities of ^{46}Ar and ^{44}S are highly depressed, and so are their central charge densities. The charge form factors of some argon and sulfur isotopes are presented, and the minima of the charge form factors shift upward and inward when the central nuclear charge distributions are more depressed. Besides, the effect of the central depression on the charge form factors is studied with a parametrized distribution, when the root-mean-square charge radii remain constant.

DOI: 10.1103/PhysRevC.82.024320 PACS number(s): 21.10.Ft, 21.60.Jz, 25.30.Bf

I. INTRODUCTION

Nuclear charge distribution is an important property for describing nuclear structure, and it can directly reflect proton distribution [1–3]. Nuclear charge distribution and charge radii are always the necessary outputs of various nuclear models, so precise and reliable determination of the distribution or radii can help us to constrain the nuclear models and their parameters. Elastic electron scattering at high energy is one of the most powerful tools for determining the nuclear charge distribution, because the electron-nucleus interaction is well understood and the scattering is weak enough to keep the nucleus undisturbed. The electron scattering off stable nuclei has provided an amount of reliable charge distribution [4–8], and the experiments for electron scattering off unstable nuclei have been taken into the agenda and will be carried out in the near future [9–14]. At present, plenty of work has been devoted to the theoretical study of the electron scattering off unstable nuclei [15–22].

Central depression of nuclear matter (proton and neutron) distribution is an interesting topic in nuclear physics. For example, as an extreme case of center-depressed nuclear density, the nuclear bubble has attracted great attention. The concept of a nuclear bubble originates from the explanation of equally spaced nuclear levels by Wilson in 1946 [23], in which the nucleus is assumed to be a thin spherical shell. From then on, the existence of a nuclear bubble has been examined with a variety of nuclear models, such as the liquid drop model, the Thomas-Fermi model, and the Hartree-Fock method [24–26]. Although different opinions on the exact position of center-depressed nuclei are obtained with different nuclear models, the explanations for central depression are always similar. Central depression is caused by Coulomb repulsion (for the depressed proton density) and the lack of s-state nucleons.

In this article, we will study the central depression of nuclear charge density distribution. The nuclear charge depression should be the consequence of the depressed proton distribution. The center-depressed proton densities of light and medium mass nuclei are mainly caused by the low occupancy of the proton s states. For example, the central proton density of ^{34}Si is evidently depressed in view of the proton $2s_{1/2}$ state being little occupied [27]. In the nuclei near the stability line, the energy level of the proton $2s_{1/2}$ state always lies between those of the $1d_{5/2}$ and $1d_{3/2}$ states. However, with the nuclei approaching the drip line, the energy level spacings can be changed, or the level sequence may be rearranged. ^{46,68}Ar are thought to be with greatly depressed central proton densities due to the level inversion of the proton $2s_{1/2}$ state [28]. ^{68}Ar is much more neutron-rich than ^{46}Ar, so it may be more difficult to produce and study ^{68}Ar in the laboratory. Here we will study the central depression of the nuclear charge density of ^{46}Ar using the relativistic mean-field theory. We will examine how the central charge densities change when the argon isotopes become more neutron rich. Similar to the case of ^{46}Ar, the central charge density of ^{44}S may also be evidently depressed, and the charge densities of some sulfur isotopes will be investigated with the relativistic mean-field theory. Besides the theoretical charge densities, the corresponding charge form factors will also be worked out with the phase shift analysis method. The form factors can be determined through elastic electron scattering experiments, and here we will examine theoretically the observable effects of nuclear charge central depression on the charge form factors.

This article is organized as follows. Section II introduces the methods for describing the nuclear charge density and the framework for obtaining the charge form factors with the phase shift analysis method. Section III presents the numerical results and discussion. At last, a summary is given.

*chuyanyun@gmail.com

II. THEORY

A. Nuclear charge density

Nuclear charge density can be described with a parametrized distribution, or it can be deduced from various nuclear models. Gaussian and Fermi types of distribution are two of the most frequently used for describing nuclear charge densities. Gaussian distribution is suitable for describing the charge densities of light nuclei, such as alpha particle, while Fermi-type distribution is more suitable for heavier nuclei. The two-parameter Fermi distribution can account for the nuclear charge radius and skin thickness, supposing the nucleus with smooth and saturated central charge density. In order to depict the central charge depression, we may use the three-parameter Fermi (3pF) distribution. The 3pF distribution takes the form [8]

$$\rho_c(r) = \frac{\rho_0(1 + wr^2/c^2)}{1 + e^{(r-c)/a}}, \tag{1}$$

where c is the half-density radius, a is the skin thickness, w ($w > 0$) affects the central density and ρ_0 is the normalization constant. The greater w is, the more depressed the central density.

Many nuclear models can generate reasonable nuclear charge density, for example, the liquid drop model, shell model, and self-consistent mean-field theory. Here we focus on the relativistic mean-field (RMF) theory with the following effective Lagrangian [29–32]:

$$\begin{aligned}\mathcal{L} = {} & \bar{\Psi}(i\gamma^\mu\partial_\mu - M)\Psi - g_\sigma\bar{\Psi}\sigma\Psi - g_\omega\bar{\Psi}\gamma^\mu\omega_\mu\Psi \\ & - g_\rho\bar{\Psi}\gamma^\mu\rho_\mu^a\tau^a\Psi + \tfrac{1}{2}\partial^\mu\sigma\partial_\mu\sigma - \tfrac{1}{2}m_\sigma^2\sigma^2 - \tfrac{1}{3}g_2\sigma^3 \\ & - \tfrac{1}{4}g_3\sigma^4 - \tfrac{1}{4}\Omega^{\mu\nu}\Omega_{\mu\nu} + \tfrac{1}{2}m_\omega^2\omega^\mu\omega_\mu + \tfrac{1}{4}c_3(\omega_\mu\omega^\mu)^2 \\ & - \tfrac{1}{4}\vec{R}^{\mu\nu}\cdot\vec{R}_{\mu\nu} + \tfrac{1}{2}m_\rho^2\vec{\rho}^\mu\cdot\vec{\rho}_\mu - \tfrac{1}{4}F^{\mu\nu}F_{\mu\nu} \\ & - e\bar{\Psi}\gamma^\mu A_\mu\tfrac{1}{2}(1-\tau^3)\Psi,\end{aligned} \tag{2}$$

with the tensor field

$$\Omega^{\mu\nu} = \partial^\mu\omega^\nu - \partial^\nu\omega^\mu, \tag{3}$$

$$\vec{R}^{\mu\nu} = \partial^\mu\vec{\rho}^\nu - \partial^\nu\vec{\rho}^\mu, \tag{4}$$

$$F^{\mu\nu} = \partial^\mu A^\nu - \partial^\nu A^\mu, \tag{5}$$

where

Ψ and M are the nucleon field and mass,
A_μ is the photon field,
m_σ, m_ω and m_ρ are the masses of σ, ω, and ρ mesons,
g_σ, g_ω, and g_ρ are the coupling coefficients between the mesons and nucleons,
g_2 and g_3 are the nonlinear coupling strengths of the σ meson, and
c_3 is the coupling coefficient of the nonlinear self-coupling of the ω field.

The motion equations of the nucleons and mesons can be derived according to the variational principle. Based on the no-sea approximation and mean-field approximation, the motion equations can be solved iteratively, and the wave functions of the nucleons can be obtained. Thus we get the nuclear matter (neutron and proton) distribution. Neglecting the contribution from neutrons, the nuclear charge density can be obtained by folding the proton charge distribution $\rho_p(\mathbf{r})$ with the single proton charge distribution $\rho^p(\mathbf{r})$ [33]

$$\rho_c(\mathbf{r}) = \int \rho_p(\mathbf{r}')\rho^p(|\mathbf{r} - \mathbf{r}'|)\,d\mathbf{r}', \tag{6}$$

with $\int \rho_c(\mathbf{r})\,d\mathbf{r} = Z$.

To measure how the central density is depressed, the depression degree is introduced as follows

$$D = \frac{\rho_{\max} - \rho_{\text{cent}}}{\rho_{\max}} \times 100\%, \tag{7}$$

where $\rho_{\max}$ is the maximum of the density and ρ_{cent} is the central density. The central density is more depressed when D is larger.

Once the nuclear charge density is obtained, the electrostatic potential between the electron and the nucleus can be determined as follows:

$$V_c(\mathbf{r}) = -\frac{e^2}{4\pi\epsilon_0}\int \frac{\rho_c(\mathbf{r}')}{|\mathbf{r} - \mathbf{r}'|}d\mathbf{r}'. \tag{8}$$

For simplicity, the nuclear charge distribution is assumed to be spherical in the following, so the electrostatic potential is also spherical.

B. Nuclear charge form factor

The elastic electron scattering by the nuclear electrostatic potential is described by the Dirac equation [34,35]

$$[\alpha\cdot\mathbf{p} + \beta m + V(\mathbf{r})]\Psi(\mathbf{r}) = E\Psi(\mathbf{r}), \tag{9}$$

where α and β are the Dirac matrices, and m, E, and $\mathbf{p}$ are the rest mass, energy, and momentum of the incident electron, respectively. When the potential $V(\mathbf{r})$ is spherical, the solution of the Dirac equation can be decomposed into different partial waves with definite orbital angular momentum and spin orientation. The phase shifts, which are characterized into spin-up ones δ_l^+ (with parallel alignment of *phl* and *phs*) and spin-down ones δ_l^- (with antiparallel alignment of **l** and **s**), can be worked out by solving the Dirac equation with scattering boundary condition [36]. Then can be determined the direct scattering amplitude

$$f(\theta) = \frac{1}{2ik}\sum_{l=0}^{\infty}[(l+1)(e^{2i\delta_l^+} - 1) + l(e^{2i\delta_l^-} - 1)]P_l(\cos\theta), \tag{10}$$

and the spin-flip scattering amplitude

$$g(\theta) = \frac{1}{2ik}\sum_{l=0}^{\infty}[e^{2i\delta_l^-} - e^{2i\delta_l^+}]P_l^1(\cos\theta), \tag{11}$$

with P_l and P_L^1 denoting the Legendre function and associated Legendre function, respectively.

The differential cross section can be calculated

$$\frac{d\sigma}{d\Omega} = |f(\theta)|^2 + |g(\theta)|^2, \tag{12}$$

TABLE I. Root-mean-square charge radii (R_c) and central depression degrees (D) of the charge densities with the 3pF distribution taking different w values.

w	R_c (fm)	D
0.0	4.10	0.0%
0.5	4.39	9.3%
1.0	4.54	23.8%

as well as the form factor

$$|F(q)|^2 = \frac{d\sigma/d\Omega}{d\sigma_M/d\Omega}, \tag{13}$$

with the momentum transfer

$$q = 2k \sin\frac{\theta}{2},$$

and Mott cross section

$$\frac{d\sigma_M}{d\Omega} = \left(\frac{Z\alpha^2}{2E}\right)^2 \frac{\cos^2\frac{\theta}{2}}{\sin^4\frac{\theta}{2}}.$$

III. NUMERICAL RESULTS AND DISCUSSION

To begin with, we study the central depression of nuclear charge density distribution with the three-parameter Fermi (3pF) distribution. ^{40}Ca is chosen as the example nucleus. The parameters in the 3pF distribution [Eq. (1)] are set in the common way, $c = 1.25A^{1/3}$ fm and $a = 0.65$ fm. The parameter w is adjustable to illustrate how the central density is depressed. Table I shows the rms radii and central depression degrees for three different values of w. $w = 0$ means no central depression. With increasing w, the central densities become more depressed and the corresponding rms radii get larger.

The charge densities for different w values are plotted in Fig. 1. The changing trend of the cental density depression is illustrated when the value of w varies. The form factors defined in Eq. (13) are displayed in Fig. 2. The charge form factors are not sensitive to the scattering energy [16], and the scattering energy is chosen to be 500 MeV (a typical beam

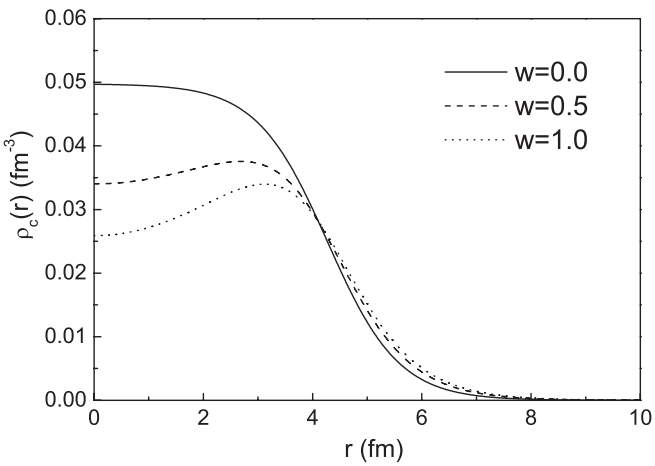

FIG. 1. Nuclear charge densities in the form of three-parameter Fermi distribution with different w values.

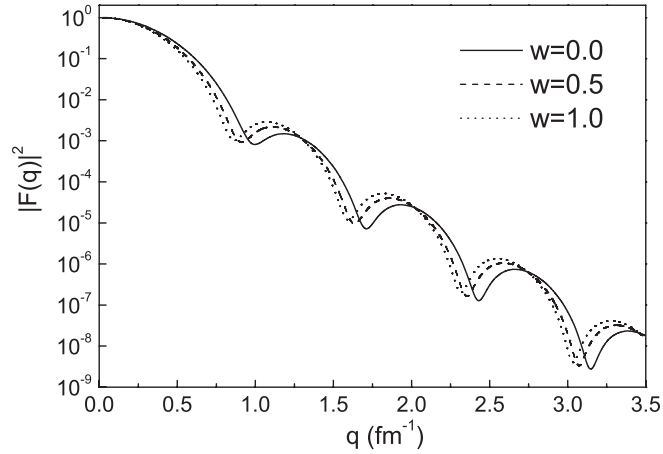

FIG. 2. Nuclear charge form factors for the charge densities in Fig. 1.

energy in high-energy electron-nucleus scattering) throughout our calculation. With w increasing, the minima of the form factors shift inward and upward, which should be caused by central depression of the nuclear charge density.

In the following, we study the central depression of nuclear charge densities of some nuclei with relativistic mean-field theory, and check whether there exist similar effects as the above case with the 3pF charge distribution. In the relativistic mean-field calculation, the BCS treatment is adopted for the open-shell nuclei, and the pairing gaps are $\Delta_n = \Delta_p = 11.2/\sqrt{A}$ MeV.

^{46}Ar is thought to be with clear center-depressed proton density [28], so its central charge density should also be evidently depressed. As is well known, the central nuclear charge density is contributed mainly from protons occupying the s state. The valence protons in ^{46}Ar prefer to occupy the $1d_{3/2}$ state rather than the $2s_{1/2}$ state, in order to obtain a lower system energy. However, this is not the case in the less neutron-rich argon isotopes, whose valence protons are more likely to occupy the $2s_{1/2}$ state instead of the $1d_{3/2}$ state. This changing tendency along the argon isotopic chain is reproduced in the relativistic mean-field calculations with NLSH and TM2 parameter sets [37,38], shown in Table II. The NLSH and TM2 parameter sets are often used in the literature. They are reliable for stable nuclei and can give reasonable description of the exotic nuclei. According to Table II, the RMF calculations can reproduce the changing tendency of the binding energies and charge radii reported in other literature [39,40], although the absolute values calculated here deviate from the referenced ones.

The probability of the valence protons occupying the $2s_{1/2}$ state gets smaller when the argon isotope becomes more neutron rich. This effect may be caused by the following phenomena. First, the potential felt by the valence protons is changed when more and more neutrons are added to the isotope, so the energy level of the proton $2s_{1/2}$ state is lifted up while that of $1d_{3/2}$ is pressed down. Second, the neutrons become more widely extended when the nucleus is more neutron rich. The strong proton-neutron interaction pulls the valence protons outward, meaning that the central proton

TABLE II. Binding energies (B/A), rms charge radii (R_c), probabilities of the valence protons occupying the $2s_{1/2}$ state (P), central charge density depression degrees (D) for argon and sulfur isotopes calculated from the RMF theory with NLSH and TM2 parameter sets, and the referenced binding energies and charge radii in other literature [39,40].

Nucleus	NLSH				TM2				Referenced data	
	B/A (MeV)	R_c (fm)	P	D	B/A (MeV)	R_c (fm)	P	D	B/A (MeV)	R_c (fm)
^{36}Ar	8.337	3.36	0.67	2.5%	8.371	3.44	0.60	11.2%	8.520	3.39
^{40}Ar	8.566	3.37	0.54	5.9%	8.589	3.45	0.48	13.4%	8.595	3.43
^{46}Ar	8.416	3.40	0.24	30.5%	8.487	3.47	0.18	40.0%	8.411	3.44
^{32}S	8.233	3.24	0.50	7.5%	8.331	3.31	0.49	12.0%	8.493	3.26
^{38}S	8.404	3.28	0.27	16.7%	8.443	3.36	0.22	23.8%	8.449	–
^{44}S	7.976	3.32	0.08	35.7%	8.052	3.40	0.05	42.2%	7.994	–

density is depressed and the valence protons are less likely to occupy the low orbital angular momentum states.

The preference for the proton $1d_{3/2}$ state rather than $2s_{1/2}$ in neutron-rich argon isotopes is also supported by the experimental evidence from chlorine and potassium isotopes [41]. The chlorine isotopes ^{33,35,37,39}Cl are determined to be in the ground state with spin-parity $J^\pi = \frac{3}{2}^+$, while ^{41,43,45}Cl with $J^\pi = \frac{1}{2}^+$. Based on the shell model, the total spin-parity of even-odd or odd-even nuclei should be contributed by the valence nucleon(s) outside an even-even core with $J^\pi = 0^+$. Spin-parity $J^\pi = \frac{3}{2}^+$ of ^{33,35,37,39}Cl means that two of the three valence protons occupy the $2s_{1/2}$ state and the last one occupies the $1d_{3/2}$ state. The case for ^{41,43,45}Cl is different, in that two of the three valence protons occupy the $1d_{3/2}$ state and the last one occupies the $2s_{1/2}$ state. The above evidence indicates that the valence protons prefer to occupy the $1d_{3/2}$ state rather than the $2s_{1/2}$ state in neutron-rich chlorine isotopes. A similar situation happens for neutron-rich potassium isotopes. We, therefore, have reason to believe that the very neutron-rich nuclei with charge numbers ranging from 16 to 19 have center-depressed central charge densities due to their low occupancy of the proton state $2s_{1/2}$.

The charge densities of ^{36,40,46}Ar from RMF theory with the NLSH parameter set are displayed in Fig. 3. It is evident that the central nuclear charge densities are more depressed when the nuclei become more neutron rich. With the above nuclear charge densities, we calculate the charge form factors defined in Eq. (13) using the partial wave analysis method. According to the charge form factors shown in Fig. 4, the minima shift upward and inward with the isotopes becoming more neutron rich. This changing trend should be caused by the variation of the nuclear charge densities, especially their central parts. The charge densities calculated with the TM2 parameter set are shown in Fig. 5, and the corresponding charge form factors are shown in Fig. 6. The results from the two parameter sets are in accordance with each other. The charge form factors can be obtained in the electron-nucleus scattering experiments. The electron scattering by stable nuclei have been measured to a high precision, and the measurement for short-lived unstable nuclei will be carried out in the next-generation facilities. Had we obtained the experimental electron-nucleus cross section, the nuclear charge densities could have been determined in a model-independent way. Then we would have compared the theoretical and experimental results so as to check the prediction of the nuclear model.

Similar to situation in ^{46}Ar, there may also exist an obvious center-depressed charge distribution in ^{44}S. According to the shell model, the two valence protons of sulfur isotopes mainly occupy the $2s1/1$ and $1d_{3/2}$ states. As we have indicated

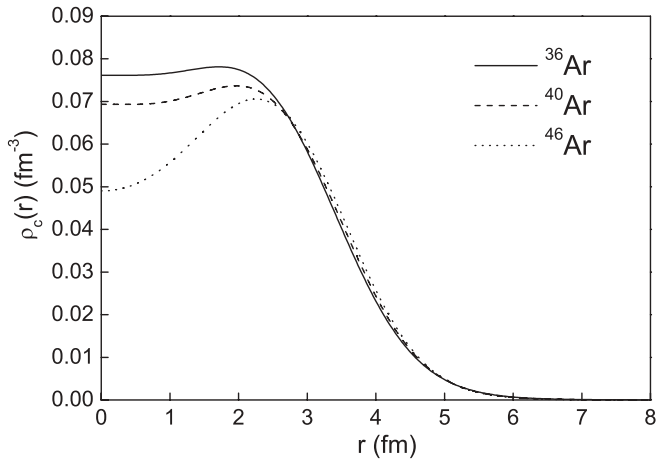

FIG. 3. Nuclear charge densities of ^{36,40,46}Ar from the RMF theory with the NLSH parameter set.

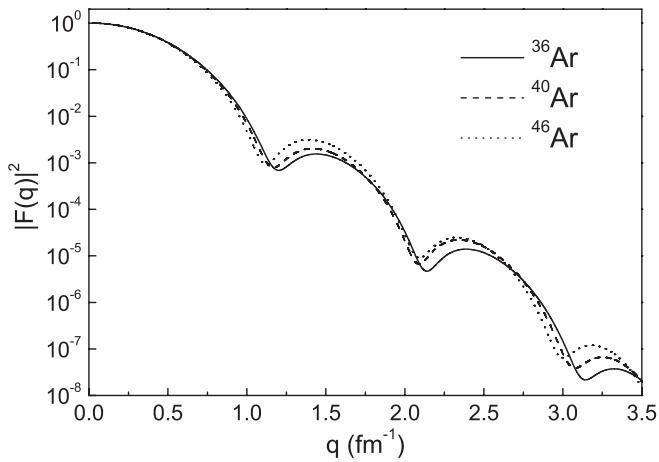

FIG. 4. Nuclear charge form factors for the charge densities in Fig. 3.

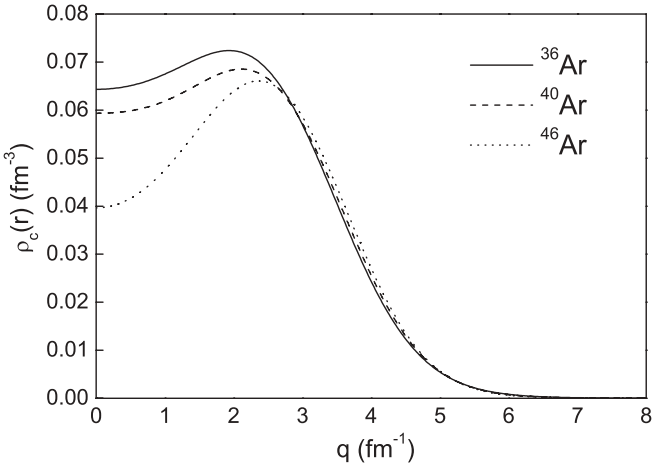

FIG. 5. Nuclear charge densities of ^{36,40,46}Ar from the RMF theory with the TM2 parameter set.

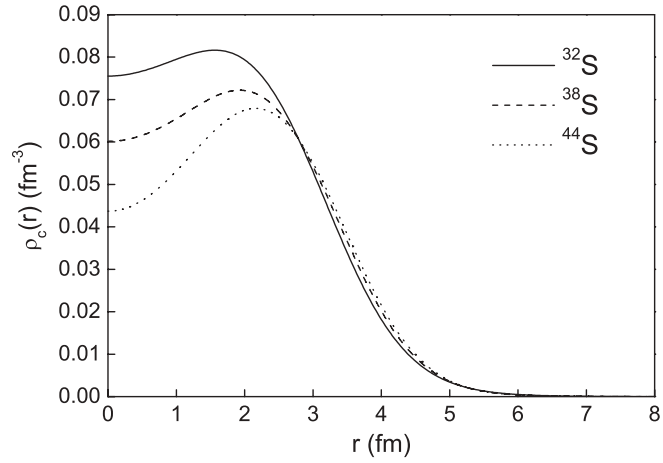

FIG. 7. Nuclear charge densities of ^{32,38,44}S from the RMF theory with the NLSH parameter set.

before, the valence protons are more likely to occupy the $1d_{3/2}$ state when the nucleus is very neutron rich. The RMF theory with NLSH and TM2 parameter sets gives the binding energies, nuclear charge radii, and the probabilities of the valence protons occupying the $2s_{1/2}$ state in Table II. The calculations well predict the changing trend of the binding energies without respect to their absolute values.

Figure 7 shows the nuclear charge densities of ^{32,38,44}S from RMF theory with the NLSH parameter set. The corresponding charge form factors are plotted in Fig. 8. The same results but with TM2 parameter set are displayed in Figs. 9 and 10. The nuclear charge densities change in a similar way as those of the argon isotopes when the nuclei become more neutron rich. The minima of the form factors shift inward and outward with the nuclei becoming more neutron rich. The changing trend of the form factors is also obtained in the case before, in which the charge densities are in the form of a 3pF distribution.

In the above cases, the central depression of nuclear charge distribution is accompanied by the increased rms charge radius. To avoid the influence of the increased charge radius on the form factors, we will study cases where the rms charge radius remains constant while increasing the central depression. ^{40}Ca is taken as the model nucleus. The charge density takes the two-parameter Fermi (2pF) form when it is not center depressed

$$\rho_c(r) \propto \frac{1}{1+e^{(r-c)/a}}, \tag{14}$$

with $c = 1.25A^{1/3}$ fm and $a = 0.65$ fm. If the central density is depressed, the charge density is simulated by subtracting a Gaussian distribution from the above 2pF distribution

$$\rho_c(r) \propto \frac{1}{1+e^{(r-c)/a}} - ge^{-r^2/t^2}, \tag{15}$$

where g is an adjustable parameter to give different depression degree, and t equals 3.3469 fm so that the rms charge radius remains constant ($R_c = 4.10$ fm) while changing the g value. The depression degree is 30% when $g = 0.5581$, and 60% when $g = 0.7888$. The charge form factors for nuclear charge densities with $D = 0\%$, 30%, and 60% are displayed in Fig. 11. According to Fig. 11, the first minimum and maximum clearly shift upward and inward, and the other minima and

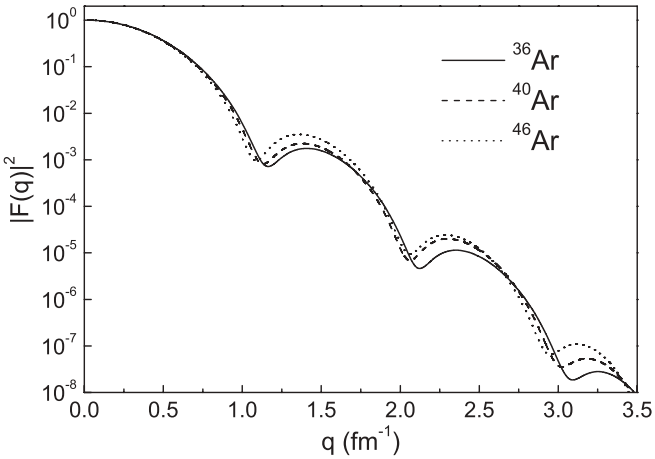

FIG. 6. Nuclear charge form factors for the charge densities in Fig. 5.

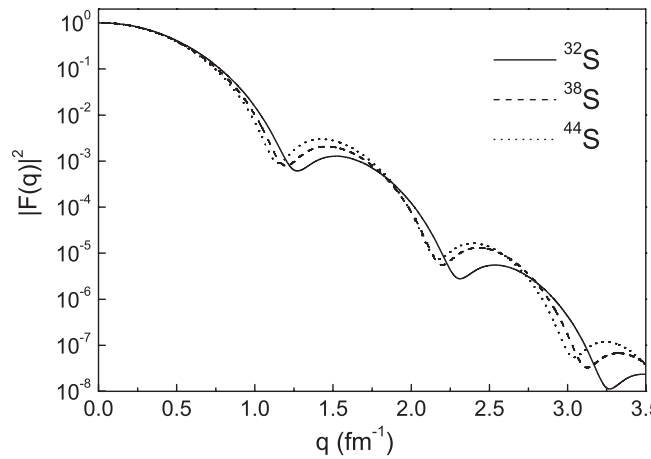

FIG. 8. Nuclear charge form factors for the charge densities in Fig. 7.

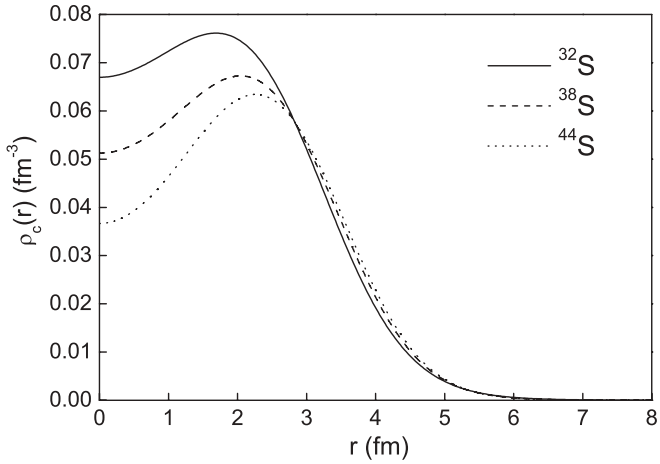

FIG. 9. Nuclear charge densities of ^{32,38,44}S from the RMF theory with the TM2 parameter set.

maxima mainly shift upward when the central charge density is depressed in this way.

According to all the above calculations, the first minima and maxima of the charge form factors shift inward and upward when the charge densities are center depressed. The first minima and maxima of the form factors lie in the region with q ranging from 0.5 to 1.5 fm^{-1}, which is covered in the planned experiments [10]. The first maximum of the form factors for the charge density with clear central depression (e.g., in Fig. 11) has a magnitude several times larger than that for the charge density with no evident depression, and the magnitude difference can be detected in future electron scattering experiments. To determine the full charge density with ambiguity of a few percent, it is necessary to measure the scattering cross section in a wide q range (e.g., $0.5 \sim 4$ fm^{-1}) with acceptable precision, and the high luminosity at least 10^{27} cm^{-2} s^{-1} is needed [10,14]. The luminosity is defined as $L = N_{\rm ion}N_e$, where $N_{\rm ion}$ is the target thickness and N_e is the electron beam current. A typical beam current is 100 mA, so the target thickness should be the order of 10^9 cm^{-2} to obtain a luminosity 10^{27} cm^{-2}s^{-1}. A large target thickness is

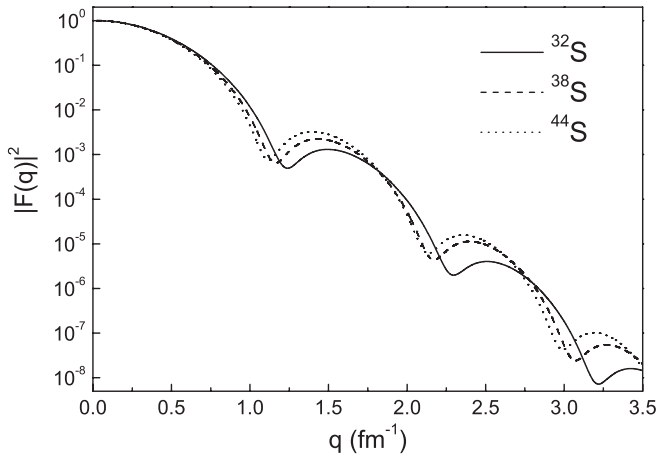

FIG. 10. Nuclear charge form factors for the charge densities in Fig. 9.

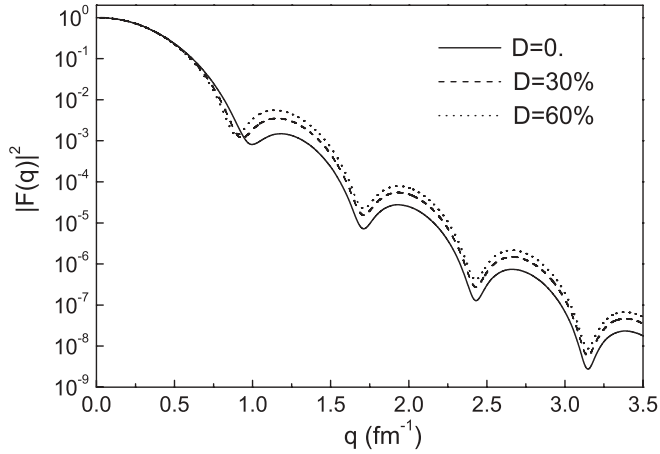

FIG. 11. Nuclear charge form factors for the differently center-depressed charge densities but with the same rms charge radius.

hard to get for very unstable nuclei. The planned experiments enable the radioactive nucleus with a half-life as short as 100 ms to be studied [13,14], so the nuclei ^{44}S and ^{46}Ar with half-lives 123 ± 10 ms and 8.4 ± 0.6 s can be studied in the future electron scattering experiments. With the development of the experimental technique, higher luminosity and higher precision measurement can be obtained for electron scattering off unstable nuclei, and the central depression of nuclear charge density can be studied through these experiments.

IV. SUMMARY

We have studied the central nuclear charge depression with the parametrized distribution and relativistic mean-field theory. The charge form factors are worked out with the partial wave analysis method. The central charge depression is depicted with the depression degree defined as the relative difference between the central and maximum charge density [Eq. (7)]. The slight central charge depression is a common phenomenon for the neutron-rich nuclei in an isotopic chain. In our previous work, the charge densities of oxygen isotopes are studied [22]. The central charge density of ^{24}O is depressed compared with that of ^{16}O, but the depression is much less clear than that in this article.

^{46}Ar is suggested to be with a clear center-depressed proton density [28]. The center-depressed proton density may be mainly caused by level inversion of the $2s_{1/2}$ and $1d_{3/2}$ states in the very neutron-rich argon isotopes. This level inversion is also supported by the evidence from the ground-state spin-parities of the very neutron-rich chlorine and potassium isotopes. According to our relativistic mean-field calculation, the central charge depression degree of ^{46}Ar is 30.5% with NLSH parameter set and 40.0% with TM2, which is obviously larger than that of ^{36,40}Ar. The charge form factors for ^{36,40,46}Ar are worked out using the partial-wave analysis method. The minima of the form factors shift upward and inward, with the isotopes becoming more neutron rich. The charge form factors can be determined in the electron-nucleus scattering experiments. At present, electron scattering experiments for stable nuclei are able to be performed with high precision,

and that for very unstable nuclei is still under construction and will be carried out in the near future. Comparing the theoretical and experimental form factors will be helpful for us to check the validity of the nuclear models and to have a better understanding of the nuclear structure.

Just as ^{46}Ar, ^{44}S may also have a clear center-depressed charge density. The charge densities and form factors of the sulfur isotopes are studied in detail, and similar conclusions as those for the argon isotopes are reached. The center-depressed nuclear charge density is an important hint of the low occupation of the *s* states by protons. Investigation of center-depressed nuclear charge distribution is helpful for us to understand the nuclear structure, such as the nuclear shell evolution in exotic nuclei.

ACKNOWLEDGMENTS

This work is supported by the National Natural Science Foundation of China (Grants 10535010, 10675090, and 10775068), by the 973 National Major State Basic Research and Development of China (Grant 2007CB815004), by CAS Knowledge Innovation Project KJCX2-SW-N02, and by the Research Fund of Doctoral Point (RFDP), No. 20070284016.

[1] R. Hofstadter, Rev. Mod. Phys. **28**, 214 (1956).
[2] T. de Forest and J. D. Walecka, Adv. Phys. **15**, 1 (1966).
[3] T. W. Donnelly and J. D. Walecka, Annu. Rev. Nucl. Part. Sci. **25**, 329 (1975).
[4] R. F. Frosch, J. S. McCarthy, R. E. Rand, and M. R. Yearian, Phys. Rev. **160**, 874 (1967).
[5] J. Heisenberg, R. Hofstadter, J. S. McCarthy, and I. Sick, Phys. Rev. Lett. **23**, 1402 (1969).
[6] I. Sick and J. S. McCarthy, Nucl. Phys. A **150**, 631 (1970).
[7] C. R. Ottermann, G. Köbschall, K. Maurer, K. Röhrich, Ch. Schmitt, and V. H. Walther, Nucl. Phys. A **436**, 688 (1985).
[8] C. W. De Jager, H. De Vries, and C. De Vries, At. Data Nucl. Data Tables **14**, 479 (1974); H. de Vries, C. W. de Jager, and C. de Vries, *ibid.* **36**, 495 (1987).
[9] I. Sick, Prog. Part. Nucl. Phys. **47**, 245 (2001).
[10] T. Suda and M. Wakasugi, Prog. Part. Nucl. Phys. **55**, 417 (2005).
[11] H. Simon, Nucl. Phys. A **787**, 102 (2007).
[12] An International Accelerator Facility for Beams of Ions and Antiprotons, GSI Report, 2006 (unpublished) [http://www.gsi.de/GSI-Future/cdr/].
[13] M. Wakasugi *et al.*, Phys. Rev. Lett. **100**, 164801 (2008).
[14] T. Suda *et al.*, Phys. Rev. Lett. **102**, 102501 (2009).
[15] A. N. Antonov, D. N. Kadrev, M. K. Gaidarov, E. Moya de Guerra, P. Sarriguren, J. M. Udias, V. K. Lukyanov, E. V. Zemlyanaya, and G. Z. Krumova, Phys. Rev. C **72**, 044307 (2005).
[16] X. Roca-Maza, M. Centelles, F. Salvat, and X. Viñas, Phys. Rev. C **78**, 044332 (2008).
[17] C. A. Bertulani, Phys. Lett. B **624**, 203 (2005).
[18] S. Karataglidis and K. Amos, Phys. Lett. B **650**, 148 (2007).
[19] Z. Wang and Z. Ren, Phys. Rev. C **70**, 034303 (2004).
[20] Z. Wang and Z. Ren, Nucl. Phys. A **794**, 47 (2007).
[21] T. Dong, Z. Ren, and Y. Guo, Phys. Rev. C **76**, 054602 (2007).
[22] Y. Chu, Z. Ren, T. Dong, and Z. Wang, Phys. Rev. C **79**, 044313 (2009).
[23] H. A. Wilson, Phys. Rev. **69**, 538 (1946).
[24] P. Siemens and H. A. Bethe, Phys. Rev. Lett. **18**, 704 (1967).
[25] W. J. Swiatecki, Phys. Scr. **28**, 349 (1983).
[26] J. Dechargé, J.-F. Berger, M. Girod, and K. Dietrich, Nucl. Phys. A **716**, 55 (2003).
[27] M. Grasso, L. Gaudefroy, E. Khan, T. Nikšić, J. Piekarewicz, O. Sorlin, N. Van Giai, and D. Vretenar, Phys. Rev. C **79**, 034318 (2009).
[28] E. Khan, M. Grasso, J. Margueron, and N. Van Giai, Nucl. Phys. A **800**, 37 (2008).
[29] C. J. Horowitz and B. D. Serot, Nucl. Phys. A **368**, 503 (1981).
[30] P. G. Reinhard, Rep. Prog. Phys. **52**, 439 (1989).
[31] P. Ring, Prog. Part. Nucl. Phys. **37**, 193 (1996).
[32] Z. Ren, A. Faessler, and A. Bobyk, Phys. Rev. C **57**, 2752 (1998).
[33] P. E. Hodgson, *Nuclear Reactions and Nuclear Structure* (Clarendon, Oxford, 1971).
[34] M. E. Rose, *Relativistic Electron Theory* (Wiley, New York, 1961).
[35] J. D. Bjorken and S. D. Drell, *Relativistic Quantum Mechanics* (McGraw-Hill, New York, 1964).
[36] F. Salvat, A. Jabalonski, and C. J. Powell, Comput. Phys. Commun. **165**, 157 (2005).
[37] M. M. Sharma, M. A. Nagarajan, and P. Ring, Phys. Lett. B **312**, 377 (1993).
[38] Y. Sugahara, H. Toki, and P. Ring, Theor. Phys. **92**, 803 (1994).
[39] G. Audi, A. H. Wapstra, and C. Thibault, Nucl. Phys. A **729**, 337 (2003).
[40] I. Angeli, At. Data Nucl. Data Tables **87**, 185 (2004).
[41] National Nuclear Data Center, Levels and Gammas database version of 6/1/2010 [http://www.nndc.bnl.gov/nudat2/indx_adopted.jsp].